Spatial correlations of Rydberg excitations in optically driven atomic ensembles

David Petrosyan
Institute of Electronic Structure and Laser, FORTH, GR-71110 Heraklion, Crete, Greece

Michael Höning and Michael Fleischhauer
Fachbereich Physik und Forschungszentrum OPTIMAS, Technische Universität Kaiserslautern, D-67663 Kaiserslautern, Germany

(Received 13 December 2012; published 28 May 2013)

We study many-body correlations in the stationary state of a continuously driven, strongly interacting dissipative system. Specifically, we examine resonant optical excitations of Rydberg states of atoms interacting via long-range dipole-dipole and van der Waals potentials employing numerical and analytical techniques. Collection of atoms within a blockade distance form a "superatom" that can accommodate at most one Rydberg excitation. The superatom excitation probability saturates to $\frac{1}{2}$ for coherently driven atoms but is significantly higher in the presence of dephasing, approaching unity as the number of atoms increases. Using the exact numerical solution of the density-matrix equations for a small system, we demonstrate that strong dephasing of the optically driven dipoles renders the many-body problem amenable to semiclassical Monte Carlo simulations. We employ the Monte Carlo algorithm for a large number of atoms and find that in the steady state of a uniformly driven, extended one-dimensional system, the saturation of superatoms leads to quasicrystallization of Rydberg excitations whose correlations exhibit damped spatial oscillations. We show that the behavior of the system under the van der Waals interaction potential can be approximated by a rate-equations model based on a "hard-rod" interatomic potential, and by solving it we obtain the period and correlation length for the density wave of Rydberg excitations.

DOI: 10.1103/PhysRevA.87.053414 PACS number(s): 32.80.Ee, 32.80.Rm, 37.10.Jk, 75.30.Fv

I. INTRODUCTION

Strong, long-range dipole-dipole (DD) or van der Waals (vdW) interactions between atoms in highly excited Rydberg states [1] can suppress multiple Rydberg excitations within a certain interaction (blockade) volume, while enhancing the rate of single collective excitation [2–10]. The resulting dipole blockade constitutes the basis for a number of promising quantum information schemes [11] and interesting many-body effects involving long-range correlations and crystallization of Rydberg excitations [12–31].

Much of the research on strongly interacting Rydberg atoms is focused on the unitary dynamics or ground state of the many-body system. In coherently driven ensembles of atoms, depending on the strength and detuning of the driving lasers, different ground-state phases with crystalline order emerge [12–17]. Yet adiabatically attaining the ground state of a large system requires exceeding preparation times [18,19] during which the decoherence and dissipation associated with the optical excitation cannot be neglected. This necessitates the consideration of open systems and their stationary states [31], which is the main purpose of this paper.

We study theoretically resonant optical excitations of Rydberg states of atoms interacting with each other via DD and vdW potentials. Atoms within a blockade distance form a "superatom" which can accommodate at most one collective Rydberg excitation [2,8,10,32–34]. We show that the steady-state excitation probability of the superatom saturates to a value of $\frac{1}{2}$ for coherently driven atoms but can be significantly higher in the presence of strong dephasing [34]. We then consider extended one-dimensional (1D) atomic ensembles and explore both the low-density (lattice) regime [25,31] with one or few atoms per blockade distance and the high-density (continuous) regime [27–30] with many atoms per blockade distance.

The theoretical treatment of the open many-body systems is a challenging task. Whereas 1D lattice systems of moderate size can be treated exactly using generalized time-dependent density-matrix renormalization group (t-DMRG) algorithms [31], the absence of a fundamental length scale (lattice constant) prevents such treatment for continuous (high-density) systems. Recently, different semiclassical Monte Carlo (MC) algorithms have been proposed and applied [30,35,36], but there has been no proof of their validity for driven many-body systems, and the accuracy of their predictions under various conditions has not been assessed. Here we present exact solutions for $N \leqslant 11$ atoms within a few blockade distances and show that under strong dephasing a semiclassical iterative MC sampling algorithm can accurately and efficiently simulate the stationary state of the system. We apply this algorithm to larger 1D systems of $N \leqslant 10^3$ atoms within 10–15 blockade distances. For the vdW interacting atoms at high densities, corresponding to the excitation probability of superatoms approaching unity, we predict a quasicrystallization of Rydberg excitations, i.e., the formation of a density wave with correlation length exceeding the blockade distance. We interpret this result as a tight packing of superatoms having rather "hard" boundaries. In contrast, the DD potential appears to be much "softer," resulting in a shorter correlation length.

To obtain analytical results for the vdW interacting atoms, we introduce a rate-equations model based on a "hard-rod" (HR) interatomic potential, similar to that used in Ref. [23]. Different from the thermodynamic treatment of unitary system of Ref. [23], our approach to the dissipative system is a dynamical one allowing us to connect the unknown parameters of the classical HR model [37] to the physical parameters of the system, such as the excitation rate of the atoms and their density. We derive the period and correlation length of the density wave and discuss the limitations of the HR model.

We also find that the DD potential is too "soft" for assigning a well-defined interaction range compatible with an approximate HR model.

This paper is organized as follows. In Sec. II we introduce the Hamiltonian and dissipative terms of the master equation for the density matrix of the many-body system and examine the properties of strongly driven superatoms in the presence or absence of dephasing. In Sec. III we study extended 1D systems; we employ the exact solution of the master equation for several atoms to determine the validity conditions of semiclassical Monte Carlo simulations which are then used to study continuous systems of hundreds of atoms. A model based on the HR interatomic potential is derived and analytically solved in Sec. IV and compared with the results of numerical simulations for the vdW interacting atoms. Experimental considerations and conclusions are summarized in Sec. V.

II. THE MANY-BODY SYSTEM

We consider an ensemble of N atoms irradiated by a uniform driving field that couples nearly resonantly the atomic ground state $|g\rangle$ to the highly excited Rydberg state $|r\rangle$ with Rabi frequency Ω [Fig. 1(a)]. A pair of atoms i and j at positions $\mathbf{x}_i$ and $\mathbf{x}_j$ excited to states $|r\rangle$ interact either via the DD ($p=3$) [38] or vdW ($p=6$) [39] potential $\hbar\Delta(\mathbf{x}_i-\mathbf{x}_j)=\hbar C_p|\mathbf{x}_i-\mathbf{x}_j|^{-p}$. In the frame rotating with the driving field frequency ω, the system Hamiltonian $\mathcal{H}=\mathcal{V}_{\rm af}+\mathcal{V}_{\rm aa}$ is

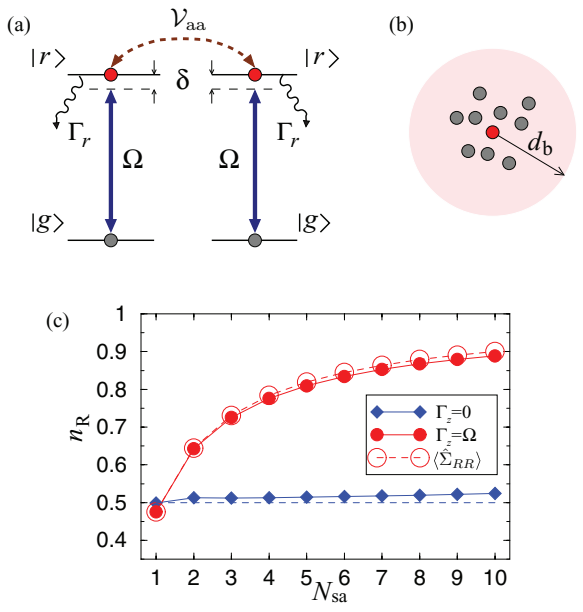

FIG. 1. (Color online) (a) Level scheme of atoms interacting with the driving field Ω on transition $|g\rangle\rightarrow|r\rangle$ with detuning δ, while $\mathcal{V}_{\rm aa}$ denotes the DD or vdW interaction between the atoms in Rydberg state $|r\rangle$ having the (population) decay rate Γ_r. (b) Atoms within the blockade distance $d_{\rm b}$ form a superatom with at most one Rydberg excitation. (c) Mean number of Rydberg excitations $n_{\rm R}$ of a superatom containing $N_{\rm sa}\leqslant 10$ atoms within $L=0.7d_{\rm b}$ (vdW interaction), obtained from the exact steady-state solutions of Eq. (1) for $\delta=0$, $\Gamma_r=0.1\Omega$, and $\Gamma_z=0$ (blue diamonds) and $\Gamma_z=\Omega$ (solid red circles). Also shown is the Rydberg excitation probability $\langle\hat{\Sigma}_{RR}\rangle$ of the superatom (open red circles) as per Eq. (4).

composed of the atom-field and atom-atom interactions, $\mathcal{V}_{\rm af}=-\hbar\sum_j^N[\delta\hat{\sigma}_{rr}^j+\Omega(\hat{\sigma}_{rg}^j+\hat{\sigma}_{gr}^j)]$ and $\mathcal{V}_{\rm aa}=\hbar\sum_{i<j}^N\hat{\sigma}_{rr}^i\Delta(\mathbf{x}_i-\mathbf{x}_j)\hat{\sigma}_{rr}^j$, where $\hat{\sigma}_{\mu\nu}^j\equiv|\mu\rangle_{jj}\langle\nu|$ is the transition ($\mu\neq\nu$) or projection ($\mu=\nu$) operator for atom j at position $\mathbf{x}_j$ and $\delta=\omega-\omega_{rg}$ is the driving field detuning. The relaxation processes affecting the atoms include the spontaneous (radiative) decay of the excited state $|r\rangle$ with rate Γ_r and the (nonradiative) dephasing of atomic coherence $\hat{\sigma}_{rg}$ with rate Γ_z; the decay rate of the Rydberg state is typically small compared to Ω, while the physical origins of dephasing include nonradiative collisions, Doppler shifts, inhomogeneous trapping potential, and the excitation laser linewidth. The decay and dephasing Liouvillians, acting independently on each atom, are given, respectively, by $\mathcal{L}_r^j\hat{\rho}=\frac{1}{2}\Gamma_r[2\hat{\sigma}_{gr}^j\hat{\rho}\hat{\sigma}_{rg}^j-\{\hat{\sigma}_{rr}^j,\hat{\rho}\}]$ and $\mathcal{L}_z^j\hat{\rho}=\Gamma_z[(\hat{\sigma}_{rr}^j-\hat{\sigma}_{gg}^j)\hat{\rho}(\hat{\sigma}_{rr}^j-\hat{\sigma}_{gg}^j)-\hat{\rho}]$ [40]. The density matrix $\hat{\rho}$ of the N-atom system obeys the master equation

$$\partial_t\hat{\rho}=-\frac{i}{\hbar}[\mathcal{H},\hat{\rho}]+\mathcal{L}\hat{\rho}, \tag{1}$$

with $\mathcal{L}\hat{\rho}=\sum_j^N(\mathcal{L}_r^j\hat{\rho}+\mathcal{L}_z^j\hat{\rho})$.

A. Blockade distance

For a single two-level atom, the steady-state population of the excited state $|r\rangle$ is a Lorentzian function of detuning δ,

$$\langle\hat{\sigma}_{rr}\rangle=\frac{\Omega^2}{2\Omega^2+\frac{\Gamma_r}{2\gamma_{rg}}\left(\gamma_{rg}^2+\delta^2\right)}, \tag{2}$$

with the width $w=\gamma_{rg}\sqrt{4\Omega^2/\Gamma_r\gamma_{rg}+1}$, where $\gamma_{rg}\equiv\frac{1}{2}\Gamma_r+2\Gamma_z$ is the total (transversal) relaxation rate of the $\hat{\sigma}_{rg}$ coherence [40]. For strong ($\Omega^2>\Gamma_r\gamma_{rg}$), resonant ($\delta\ll w$) driving, the population saturates to $\langle\hat{\sigma}_{rr}\rangle\rightarrow\frac{1}{2}$. But given an atom in the Rydberg state $|r\rangle$, it will induce a level shift Δ, equivalent to detuning δ, of another atom, blocking its Rydberg excitation when $\Delta\gtrsim w$. This is the essence of the dipole blockade [2,10,11]. We may therefore define the blockade distance $d_{\rm b}$ via $\Delta(d_{\rm b})=w$, which yields

$$d_{\rm b}\equiv\sqrt[p]{\frac{C_p}{w}}\simeq\left(\frac{C_p}{2\Omega}\sqrt{\frac{\Gamma_r}{\gamma_{rg}}}\right)^{1/p}, \tag{3}$$

with $p=3$ for the DD interaction and $p=6$ for the vdW interaction.

B. The superatom

Consider $N_{\rm sa}$ atoms within the distance $L<d_{\rm b}$, such that $\Delta(\mathbf{x}_i-\mathbf{x}_j)\gg w$ for any pair of atoms i and j [Fig. 1(b)]. We thus expect that the superatom can accommodate at most one Rydberg excitation [32,33]. This is confirmed by our exact numerical simulations for $N_{\rm sa}\leqslant 10$; starting with all the atoms in the ground state $|g\rangle$, we propagate Eq. (1) for time t ($\gg\Omega^{-1}$) long enough until the steady state is reached. In Fig. 1(c) we show the resulting mean number of Rydberg excitations $n_{\rm R}=\langle\sum_j^{N_{\rm sa}}\hat{\sigma}_{rr}^j\rangle$ within the superatom. Clearly, $n_{\rm R}<1\,\forall\,N_{\rm sa}$, while we verify that the probabilities of double $\langle\hat{\sigma}_{rr}^i\hat{\sigma}_{rr}^j\rangle$, triple $\langle\hat{\sigma}_{rr}^i\hat{\sigma}_{rr}^j\hat{\sigma}_{rr}^k\rangle$, etc., excitations are always small.

In the absence of dephasing, $\Gamma_z = 0$ and $\gamma_{rg} = \frac{1}{2}\Gamma_r \ll \Omega$, we have $n_R \simeq \frac{1}{2}$ independent of N_{sa}. The ground state $|G\rangle = |g_1, g_2, \ldots, g_{N_{sa}}\rangle$ of the superatom is coupled only to the single collective Rydberg excitation state $|R^{(1)}\rangle = \frac{1}{\sqrt{N_{sa}}} \sum_j^{N_{sa}} |g_1, g_2, \ldots, r_j, \ldots, g_{N_{sa}}\rangle$, while all the states $|R^{(n)}\rangle$ with a higher number $n > 1$ of Rydberg excitations are shifted out of resonance by the strong interatomic interaction $\mathcal{V}_{aa}$ and therefore are not populated. As the collective Rabi frequency $\sqrt{N_{sa}}\Omega$ saturates the transition $|G\rangle \leftrightarrow |R^{(1)}\rangle$, the superatom ground and excited states acquire populations $\langle \hat{\Sigma}_{GG} \rangle \simeq \langle \hat{\Sigma}_{RR} \rangle \simeq \frac{1}{2}$, where $\hat{\Sigma}_{GG} \equiv \prod_{j=1}^{N_{sa}} \hat{\sigma}_{gg}^j$ and $\hat{\Sigma}_{RR} \equiv \sum_{j=1}^{N_{sa}} \hat{\sigma}_{rr}^j \prod_{i \neq j}^{N_{sa}} \hat{\sigma}_{gg}^i$ are projectors onto the ground and single Rydberg excitation states of N_{sa} atoms. We note that n_R slightly larger than $\frac{1}{2}$ seen in Fig. 1(c) is due to an imperfect blockade of Rydberg excitation [$\Delta(L) \sim 10w$] of atoms at the boundaries of the region of finite size ($L = 0.7d_b$).

Remarkably, strong dephasing Γ_z increases the mean number of Rydberg excitations $n_R > \frac{1}{2}$ within the superatom [34]. The transversal relaxation $\gamma_{rg} \gtrsim \Omega$ destroys the inter- and intra-atomic coherences, causing individual atoms to behave independently. In the basis of collective singly excited states, this corresponds to a coupling of the symmetric state $|R^{(1)}\rangle$ to all the nonsymmetric states [34]. The superatom still contains at most one Rydberg excitation, $\hat{\Sigma}_{GG} + \hat{\Sigma}_{RR} = \mathbb{1}$, which, upon combining with $\hat{\sigma}_{gg}^j + \hat{\sigma}_{rr}^j = \mathbb{1}$, yields

$$\langle \hat{\Sigma}_{RR} \rangle = \frac{N_{sa} \langle \hat{\sigma}_{rr} \rangle}{(N_{sa} - 1)\langle \hat{\sigma}_{rr} \rangle + 1}, \tag{4}$$

where $\langle \hat{\sigma}_{rr} \rangle$ is given by Eq. (2). For $N_{sa} = 1$ we have $\langle \hat{\Sigma}_{RR} \rangle = \langle \hat{\sigma}_{rr} \rangle$, as it should, while $N_{sa} \gg 1/\langle \hat{\sigma}_{rr} \rangle$ leads to $\langle \hat{\Sigma}_{RR} \rangle \to 1$. In Fig. 1(c) we plot $\langle \hat{\Sigma}_{RR} \rangle$, which reproduces well the exact numerical solution, $n_R \simeq \langle \hat{\Sigma}_{RR} \rangle$, under the same conditions.

III. EXTENDED 1D SYSTEM

We next consider the steady-state distribution of Rydberg excitations in a 1D system of $N = \rho_{at} L$ atoms of linear density ρ_{at}. For an arbitrary pattern of interatomic interactions, exact numerical solution of the many-body master equation is possible only for a relatively small number of atoms, $N \sim 10$. On the other hand, for a lattice with short-range (e.g., nearest-neighbor) interactions, the t-DMRG algorithm generalized to open quantum systems permits exact simulations for $N \sim 10^2$ atoms [31]. Unfortunately, t-DMRG is not applicable to dense systems lacking an intrinsic length scale, e.g., many atoms per interaction (blockade) range. Below we present a semiclassical Monte Carlo algorithm that can efficiently simulate large systems of $N \sim 10^3$ or more atoms. We note related algorithms employed in [30,35,36]. There is, however, no formal justification for the applicability of MC simulations to the dissipative many-body systems. We will therefore compare exact solutions of the master equation with the results of semiclassical MC simulations to establish the conditions of their validity for small but nontrivial number of atoms.

A. Monte Carlo algorithm

The dephasing suppresses interatomic coherences and disentangles the atoms, admitting only classical N-body correlations. Each atom then behaves as a driven two-level system of Eq. (2) but with the detuning δ determined by operator $\hat{S}_j \equiv \sum_{i \neq j}^{N} \hat{\sigma}_{rr}^i \Delta(\mathbf{x}_i - \mathbf{x}_j)$, which describes the total interaction-induced shift of level $|r\rangle$ for an atom at position $\mathbf{x}_j$ involving the contributions of all the Rydberg atoms $\hat{\sigma}_{rr}^i$ at positions $\mathbf{x}_i$.

The suppression of entanglement between the atoms prompts us to introduce an efficient procedure to simulate the stationary distribution of Rydberg excitation probabilities at any atomic density ρ_{at}. Our algorithm relies on iterative MC sampling of $\{\hat{\sigma}_{rr}^j\}$ for an ensemble of N atoms, in the spirit of the Hartree-Fock method. We start with, e.g., all the atoms in the ground state, $\langle \hat{\sigma}_{gg}^j \rangle = 1 \; \forall \; j \in [1, N]$, although the resulting steady state does not depend on the initial configuration. At every step, for each atom j, we draw a uniform random number $s \in [0,1]$ and compare it with the Rydberg state population $\langle \hat{\sigma}_{rr}^j \rangle$; if $s \leqslant \langle \hat{\sigma}_{rr}^j \rangle$, we set $\hat{\sigma}_{rr}^j \to 1$; otherwise, $\hat{\sigma}_{rr}^j \to 0$. In turn, the thus constructed binary configuration of Rydberg excitations $\{\hat{\sigma}_{rr}^i\} \to \{0,1,0,0, \ldots\}$ determines the level shift $\hat{S}_j$ (equivalent to detuning δ) of atom j when evaluating $\langle \hat{\sigma}_{rr}^j \rangle$. We continuously iterate this procedure, sifting repeatedly through every atom in the potential generated by all the other atoms in a self-consistent way. The probability distribution $\bar{\sigma}_{rr}^j$ of Rydberg excitations results from averaging over many ($\sim 10^6$) configurations $\{\hat{\sigma}_{rr}^j\}$.

B. Small system

We have performed exact numerical simulations of the master equation (1) for $N \leqslant 11$ atoms with and without dephasing Γ_z. In Fig. 2 we show the stationary populations $\langle \hat{\sigma}_{rr}^j \rangle$ of Rydberg states of vdW interacting atoms in a lattice of length $L = 3d_b$ [open boundary conditions (OBC)]. When the interatomic distance exceeds d_b ($N = 3$), interactions play no role, and the population $\langle \hat{\sigma}_{rr}^j \rangle$ for each atom is given by Eq. (2). With increasing atomic density, interactions progressively suppress the Rydberg state populations of individual atoms. Simultaneously, we observe an onset of the density wave of Rydberg excitations $\langle \hat{\sigma}_{rr}^j \rangle$.

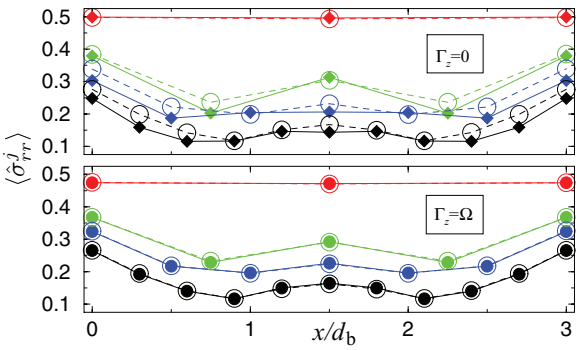

FIG. 2. (Color online) Rydberg state populations $\langle \hat{\sigma}_{rr}^j \rangle$ of $N = 3$, 5,7,11 atoms (from top to bottom: red, green, blue, black) in a 1D lattice of length $L = 3d_b$ (vdW interaction) obtained from the exact solutions of Eq. (1) for $\delta = 0$, $\Gamma_r = 0.1\Omega$, and (top) $\Gamma_z = 0$ and (bottom) $\Gamma_z = \Omega$. Also shown are the corresponding Rydberg excitation probabilities $\bar{\sigma}_{rr}^j$ (open circles) obtained from MC simulations.

We can now compare the exact solution with the predictions of semiclassical MC simulations. In Fig. 2 we plot $\bar{\sigma}_{rr}^{j}$ for various N and verify that, for strong dephasing ($\Gamma_z = \Omega$), the MC algorithm accurately reproduces the exact steady-state populations $\langle\hat{\sigma}_{rr}^{j}\rangle$. In the absence of dephasing ($\Gamma_z = 0$), however, the steady state resulting from the MC simulations deviates substantially from the exact state of the system: for the relative error $\delta\sigma_{rr}^{j} \equiv \frac{|\langle\hat{\sigma}_{rr}^{j}\rangle - \bar{\sigma}_{rr}^{j}|}{\langle\hat{\sigma}_{rr}^{j}\rangle}$ and its average over all the atoms $\overline{\delta\sigma}_{rr} \equiv \frac{1}{N}\sum_{j}^{N}\delta\sigma_{rr}^{j}$ we have $\max[\delta\sigma_{rr}^{j}] \simeq 0.26$ and $\overline{\delta\sigma}_{rr} \simeq 0.14$. Hence, neglecting the interatomic coherences, as implied by the semiclassical MC algorithm, is an uncontrolled approximation in the absence of dephasing. Then the MC simulations cannot be relied upon for obtaining the important characteristics of the system, such as the period and correlation length of the Rydberg excitation density wave.

C. Large system

We employ the above MC procedure to study realistically large 1D systems of up to $N \sim 10^3$ atoms interacting via the DD and vdW interactions and subject to strong dephasing. In Fig. 3(a) we show the spatial distribution of Rydberg excitation probabilities in a finite system of length $L = 15d_{\rm b}$ (OBC) for different atomic densities. Interactions between the atoms suppress the Rydberg excitation probabilities $\bar{\sigma}_{rr}^{j}$, and the suppression is stronger the higher the atomic density is (smaller interatomic distance) and the stronger the interaction

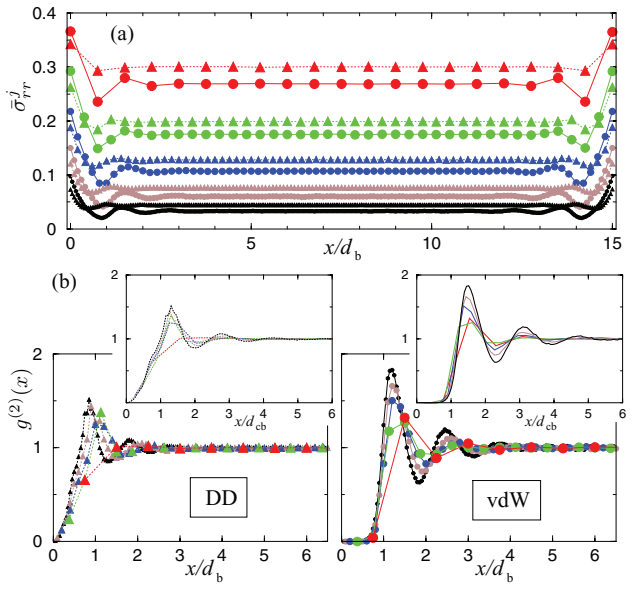

FIG. 3. (Color online) (a) Probabilities $\bar{\sigma}_{rr}^{j}$ of Rydberg excitations in a 1D atomic ensemble of length $L = 15d_{\rm b}$ (OBC) obtained from MC simulations with $\delta = 0$, $\Gamma_r = 0.1\Omega$, and $\Gamma_z = \Omega$. Triangles (connected by dotted lines) correspond to the DD interaction, and circles (connected by solid lines) correspond to the vdW interaction between the atoms. The atomic densities are, from top to bottom, $\rho_{\rm at}d_{\rm b} = 1\frac{1}{3}, 2\frac{2}{3}, 5, 10, 20$ (red, green, blue, brown, black). (b) The corresponding 1D spatial correlations $g^{(2)}(x)$ of Rydberg excitations of (left) DD and (right) vdW interacting atoms. In the inset of each graph, $g^{(2)}(x)$ is plotted vs x in units of the corresponding collective blockade distance $d_{\rm cb}$ of Eq. (5).

is. The Rydberg excitations are then repelled to the boundaries of the system. An atom at the edge, having a higher probability to be excited, suppresses the excitation of the neighboring atoms within the blockade distance, beyond which another atom acquires a higher excitation probability. Hence a Rydberg excitation density wave develops. This behavior is significantly more pronounced for the vdW interaction between the atoms, which is stronger within the blockade distance but falls off fast outside of it, compared to the DD interaction, which is weaker at short distances and has longer tails. The vdW potential is thus more reminiscent of a hard-rod interaction, while the DD potential is much softer.

From many configurations $\{\hat{\sigma}_{rr}^{j}\}$, we can extract the spatial correlations of Rydberg excitations $G^{(2)}(x \equiv |\mathbf{x}_i - \mathbf{x}_j|) = \overline{\hat{\sigma}_{rr}^{i}\hat{\sigma}_{rr}^{j}}$. More explicitly, we place a Rydberg atom ($\hat{\sigma}_{rr}^{i} = 1$) at the origin $\mathbf{x}_i = 0$ and then use the above MC procedure to calculate $\bar{\sigma}_{rr}^{j}\,\forall\,\mathbf{x}_j > 0$, from which we obtain the normalized correlation function as $g^{(2)}(x) = \bar{\sigma}_{rr}^{j}/\bar{\sigma}_{rr}$, where $\bar{\sigma}_{rr} = \frac{1}{N}\sum_{j=1}^{N}\bar{\sigma}_{rr}^{j}$ is the spatial average with $N \gg 1$ ($L \gg d_{\rm b}$). In Fig. 3(b) we show the corresponding $g^{(2)}(x)$ for the DD and vdW interactions. In the case of vdW interaction, the Rydberg atom at $x = 0$ almost completely blocks the excitation of all the atoms within the blockade distance $x \lesssim d_{\rm b}$. In contrast, for the DD potential the excitation blockage is only partial as $g^{(2)}(x)$ grows nearly linearly in the region of $x < d_{\rm b}$. In addition, for higher atomic densities $\rho_{\rm at}d_{\rm b} > 5$, we observe damped spatial oscillations of $g^{(2)}(x)$ with increasing amplitude and slowly decreasing period λ close to $d_{\rm b}$.

D. Collective blockade distance

In a dense system, $\rho_{\rm at}d_{\rm b} \gg 1$, an atom in the Rydberg state $|r\rangle$ blocks the excitation of other atoms within a certain distance which, due to collective effects, is somewhat smaller than the blockade distance $d_{\rm b}$ for a pair of atoms, Eq. (3). To estimate the collective blockade distance $d_{\rm cb}$, note that the collective Rabi frequency $\Omega_{\rm cb} = \sqrt{N_{\rm cb}}\Omega$, and thereby the excitation linewidth $w_{\rm cb} \simeq 2\Omega_{\rm cb}\sqrt{\gamma_{rg}/\Gamma_r}$, for $N_{\rm cb} = \rho_{\rm at}d_{\rm cb}$ atoms is enhanced by a factor of $\sqrt{N_{\rm cb}}$ [11,12]. Substituting $N_{\rm cb}$ into the definition of $d_{\rm cb} \equiv \sqrt[p]{C_p/w_{\rm cb}}$ yields

$$d_{\rm cb} = \left(\frac{C_p}{\sqrt{\rho_{\rm at}}w}\right)^{2/(2p+1)} = \frac{d_{\rm b}}{(\rho_{\rm at}d_{\rm b})^{1/(2p+1)}}, \qquad (5)$$

with $p = 3$ for DD and $p = 6$ for vdW interactions. In turn, the number of atoms within the collective blockade distance is $N_{\rm cb} = (\rho_{\rm at}d_{\rm b})^{2p/(2p+1)}$.

In the insets of Fig. 3(b) we plot the correlation functions $g^{(2)}(x)$ with x rescaled by the corresponding (density-dependent) collective blockade distance $d_{\rm cb}$. For vdW interaction, all the curves for different atomic densities then exhibit the same oscillation period $\lambda \simeq 1.75d_{\rm cb}$.

The average (background) density of Rydberg excitations $\bar{\rho}_{\rm vdW} = \rho_{\rm at}\bar{\sigma}_{rr}$ can also be deduced from the collective excitation picture [13,29]. For the average probability of the Rydberg state of vdW interacting atoms we obtain

$$\bar{\sigma}_{rr} \approx \frac{\langle\hat{\Sigma}_{RR}\rangle}{N_{\rm sa}} = \frac{\langle\hat{\sigma}_{rr}\rangle}{(N_{\rm sa}-1)\langle\hat{\sigma}_{rr}\rangle + 1}, \qquad (6)$$

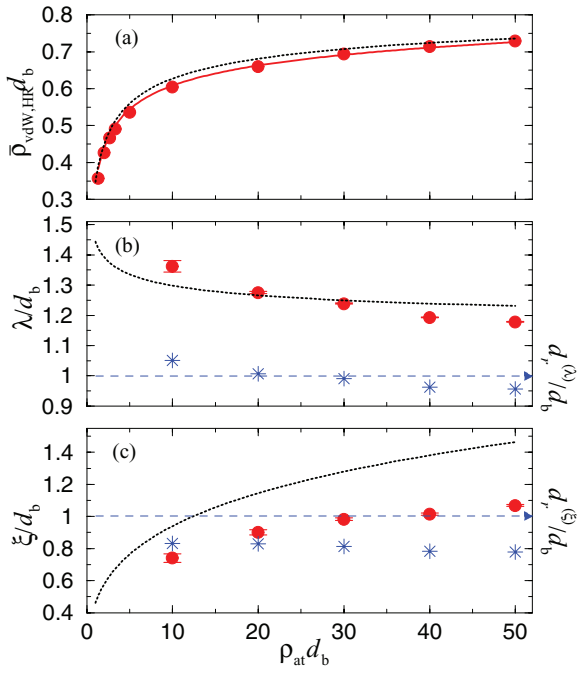

FIG. 4. (Color online) (a) Average density $\bar{\rho}_{\rm vdW} = \rho_{\rm at}\bar{\sigma}_{rr}$ of Rydberg excitations of vdW interacting atoms vs the atom density $\rho_{\rm at}$ obtained from MC simulations (circles) and Eq. (6) (solid red line). Also shown is the average excitation density $\bar{\rho}_{\rm HR}$ of Eq. (10) for the HR potential of the range $d_{\rm r} = d_{\rm b}$ (dotted black line). (b) Oscillation period λ and (c) decay length ξ of spatial correlations of excitations $g^{(2)}(x)$ vs the atom density $\rho_{\rm at}$. For the vdW interaction potential, the data points (red circles with uncertainty) are extracted from the MC simulations; for HR potential, λ and ξ are obtained from the solution of Eq. (15). The effective range $d_{\rm r}^{(\lambda,\xi)}$ (blue stars, right vertical axes) of the HR potential is obtained by equating λ and ξ for the vdW and HR interactions.

where $N_{\rm sa} \approx 1.83(\rho_{\rm at} d_{\rm b})^{12/13} \sim 2N_{\rm cb}$ is the effective number of atoms per superatom [see Fig. 4(a)]. Note that superatoms overlap.

IV. HARD-ROD POTENTIAL MODEL

We now introduce an analytical model to understand the emergence of spatial correlations of Rydberg excitations for the vdW interacting atoms. The almost-complete blockade of simultaneous excitation of two or more atoms within a distance close to $d_{\rm b}$ suggests an analogy between the vdW interaction potential and a HR potential of a range $d_{\rm r} \sim d_{\rm b}$, as was proposed in Ref. [23] for a unitary Rydberg lattice gas. The steady state of Ref. [23] was obtained from thermodynamic considerations as a state of maximum entropy. Here we present a rate-equations model with a HR potential and relate its parameters to the physical quantities of the system. We derive the steady state of the model and provide quantitative comparison of its predictions with the result of numerical simulations for vdW interacting atoms at high densities.

A. Rate-equations model

In Ref. [31] we introduced a rate-equations treatment of the 1D system with complete blockade of Rydberg excitations of neighboring atoms. We now extend this formalism to the longer-range interatomic interactions. To this end, we consider N atoms on a lattice, with one atom per site, and assume that the atoms excited to the Rydberg state $|r\rangle$ interact via the HR potential of range $d_{\rm r}$: $\Delta(\mathbf{x}_i - \mathbf{x}_j) = C_\infty \Theta(|\mathbf{x}_i - \mathbf{x}_j| - d_{\rm r})$, with $C_\infty \gg w$ and $\Theta(x)$ being the step function. An atom in state $|r\rangle$ blocks the excitation of $N_{\rm r} = \rho_{\rm at} d_{\rm r}$ neighboring atoms on both sides along the chain. For each atom, we then have two incoherent processes: a pump from $|g\rangle$ to $|r\rangle$ with rate P, conditioned upon the absence of Rydberg excitations within the range $d_{\rm r}$, $\hat{L}_{\rm p}^j = \sqrt{P}\,\hat{\sigma}_{rg}^j \prod_{|x_i - x_j| \le d_{\rm r}} (\hat{\sigma}_{rr}^i - \mathbb{1})$, and a deexcitation from $|r\rangle$ to $|g\rangle$ with rate D, $\hat{L}_{\rm d}^j = \sqrt{D}\,\hat{\sigma}_{gr}^j$. The ratio of the two rates $\kappa \equiv \frac{P}{D} = \frac{\langle\hat{\sigma}_{rr}\rangle}{1-\langle\hat{\sigma}_{rr}\rangle}$ is obtained from Eq. (2) with $\delta = 0$ as

$$\kappa = \frac{|\Omega|^2}{|\Omega|^2 + \frac{1}{2}\Gamma_r \gamma_{rg}}. \tag{7}$$

The density operator of the system obeys the equation of motion

$$\partial_t \hat{\rho} = \sum_j \left(2\hat{L}_{\rm p}^j \hat{\rho} \hat{L}_{\rm p}^{j\dagger} - \left\{\hat{L}_{\rm p}^{j\dagger}\hat{L}_{\rm p}^j, \hat{\rho}\right\} + 2\hat{L}_{\rm d}^j \hat{\rho} \hat{L}_{\rm d}^{j\dagger} - \left\{\hat{L}_{\rm d}^{j\dagger}\hat{L}_{\rm d}^j, \hat{\rho}\right\}\right). \tag{8}$$

After sufficient relaxation time, the density matrix attains a classical form, $\hat{\rho} = \sum_{\{\mu_j\}} p(\{\mu_j\})\, |\{\mu_j\}\rangle\langle\{\mu_j\}|$, where $p(\{\mu_j\})$ is the probability of the N-atom configuration $\{\mu_j\} \in (g,r)^N$. In the steady state of the system, we have the detailed balance relation

$$\frac{p(\{\mu_j\})}{p(\{\mu'_j\})} = \kappa^{M-M'}, \tag{9}$$

where $M \equiv \langle\{\mu_j\}| \sum_j \hat{\sigma}_{rr}^i |\{\mu_j\}\rangle$ is the total number of excitations in $\{\mu_j\}$. States with the same number of excitations M have equal weight, and the partition function is given by $Z_N = \sum_{M=0}^N \Lambda(M,N)\kappa^M$, where $\Lambda(M,N) = \binom{N - N_{\rm r}(M-1)}{M}$ is the number of possible arrangements of M excitations on a lattice of N sites, with any two excitations separated by at least $N_{\rm r}$ sites. The mean number of excitations is given by $\bar{M} = \frac{1}{Z_N}\sum_{M=0}^N \Lambda(M,N)\kappa^M$ while the average (background) density is $\bar{\rho}_{\rm HR} = \bar{M}/N$. In a large system $N \gg N_{\rm r}$, $\Lambda(M,N)\kappa^M$ is a highly peaked function of M; finding its maximum at $M_{\max} \simeq \bar{M}$, we obtain the density

$$\bar{\rho}_{\rm HR} = \frac{1}{d_{\rm r}} \frac{W(\beta)}{1 + W(\beta)}, \tag{10}$$

where $\beta = \kappa N_{\rm r}$ and $W(\beta)$ is the Lambert function defined via $We^W = \beta$. For $\beta \gg 1$, the density approaches $\bar{\rho}_{\rm HR} \to 1/d_{\rm r}$. We note that Eq. (10) is also obtained in the classical model of hard rods [37], where $d_{\rm r}$ is the rod length and β is a free parameter. In contrast, our derivation yields

$$\beta = \kappa \rho_{\rm at} d_{\rm r}, \tag{11}$$

which is uniquely determined through the system parameters.

Next to the boundary at $x = 0$, the density of excitations reads

$$\rho_{\rm HR}(x) = \frac{W(\beta) e^{-W(\beta)x/d_{\rm r}}}{d_{\rm r}} \sum_{k=0}^{\infty} \Theta(x/d_{\rm r} - k) \frac{\beta^k (x/d_{\rm r} - k)^k}{k!}, \tag{12}$$

and the spatial correlations are given by $g^{(2)}(x) = \rho_{\rm HR}(x - d_{\rm r})/\bar{\rho}_{\rm HR}$. Using the Laplace transform, we find that the long-distance ($x > d_{\rm r}$) correlations have the form of decaying spatial oscillations,

$$g^{(2)}(x) \simeq 1 + A\cos(2\pi x/\lambda + \phi)e^{-x/\xi}, \tag{13}$$

where the oscillation period and decay length,

$$\lambda = d_{\rm r}\frac{2\pi}{b}, \tag{14a}$$

$$\xi = d_{\rm r}\ln^{-1}\left(\frac{-b}{W(\beta)\sin(b)}\right), \tag{14b}$$

are determined by the solution of the transcendental equation for b,

$$\ln[W(\beta)] + W(\beta) - \ln\left(\frac{-b}{\sin(b)}\right) + \frac{b}{\tan(b)} = 0. \tag{15}$$

Numerical solution of Eq. (15) reveal monotonous, but slow (logarithmic), growth of ξ with increasing atomic density. For two-level atoms, $\kappa \leqslant 1$, at large but realistic densities, $\rho_{\rm at}d_{\rm b} \gtrsim 10^2$, a correlation length of a few oscillation periods can be reached.

B. Comparison of the vdW and HR potentials

To quantify the suitability of the HR model to the description of the system under the vdW potential, we now compare the mean densities of excitations $\bar{\rho}_{\rm vdW,HR}$, as well as the oscillation periods λ and decay lengths ξ of spatial correlations $g^{(2)}(x)$.

Since we need to specify the range of the HR potential, let us first equate it to the blockade distance of the vdW potential, $d_{\rm r} = d_{\rm b}$. The average densities of excitations are then remarkably close, $\bar{\rho}_{\rm vdW} \simeq \bar{\rho}_{\rm HR}$, especially at high atomic densities $\rho_{\rm at}d_{\rm b} \gg 1$; see Fig. 4(a). The oscillation period λ of the density wave is also well reproduced by the HR model [Fig. 4(b)]. With increasing atomic density, however, the period λ decreases slightly faster for the vdW potential; apparently, the superatoms having soft boundaries can pack closer to each other than permitted by the HR potential. The same softness of the vdW potential, compared to the HR potential, is the reason for somewhat shorter correlation lengths ξ; see Fig. 4(c).

Next, we may relax the assumption $d_{\rm r} = d_{\rm b}$ but take equal oscillation periods λ for both potentials and then deduce the corresponding range $d_{\rm r}^{(\lambda)}$ of the HR potential, which turns out to be close to $d_{\rm b}$ but slowly decreasing with increasing atomic density $\rho_{\rm at}$ [Fig. 4(b)]. Alternatively, we equate the correlation lengths ξ and find a somewhat smaller corresponding range of the HR potential, $d_{\rm r}^{(\xi)} \simeq 0.8d_{\rm b}$, again slowly decreasing with increasing atomic density $\rho_{\rm at}$ [Fig. 4(c)].

Finally, we have performed MC simulations for $N \gg 1$ strongly driven atoms interacting via the HR potential. In Fig. 5 we compare the correlation functions $g^{(2)}(x)$ obtained from our simulations and the corresponding analytic solutions with the results for the vdW interacting atoms under otherwise identical conditions. We observe qualitatively similar behavior when the range $d_{\rm r}$ of the HR potential is equal to the blockade distance $d_{\rm b}$ of the vdW potential. Alternatively, we may associate the range of the HR potential $d_{\rm r}$ with the collective

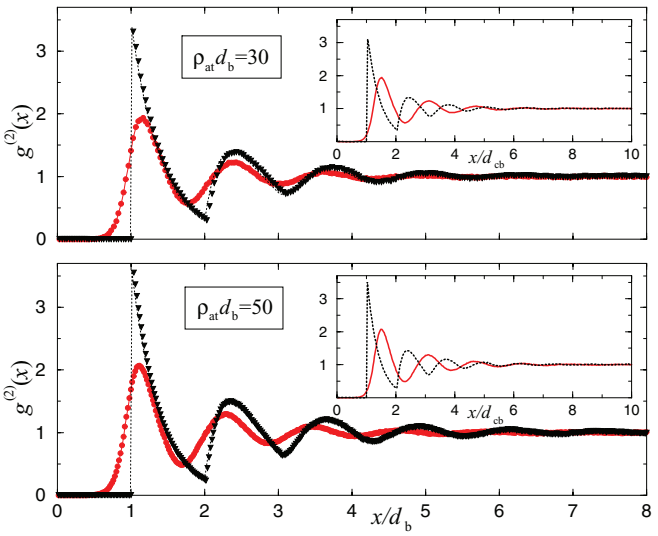

FIG. 5. (Color online) Correlations $g^{(2)}(x)$ of atomic excitations for vdW (circles) and HR (triangles) potentials obtained from MC simulations with atom densities (top) $\rho_{\rm at}d_{\rm b} = 30$ and (bottom) $\rho_{\rm at}d_{\rm b} = 50$. In the insets, $g^{(2)}(x)$ are plotted vs x in units of the collective blockade distance $d_{\rm cb}$. Atomic parameters are as in Fig. 3.

blockade distance $d_{\rm cb}$, as was done in Ref. [23], in which case $\beta = \kappa N_{\rm cb} = \kappa(\rho_{\rm at}d_{\rm b})^{12/13}$. As seen in the insets of Fig. 5, the correlation functions for the vdW and HR potentials are now considerably different, the corresponding oscillation periods being an approximately constant $\lambda \simeq 1.75d_{\rm cb}$ for the vdW potential and a slowly varying $\lambda \simeq 1.3$–$1.25d_{\rm cb}$ for the HR potential. Hence we conclude that assuming the range of the HR potential $d_{\rm r}$ to be equal to the blockade distance $d_{\rm b}$ of the vdW potential results in a more accurate description of the vdW interacting gas of atoms by the HR model. However, no fixed range $d_{\rm r}$ of the HR model can give quantitatively correct predictions of the oscillation period and decay length of spatial correlations of Rydberg excitations of the vdW interacting atoms.

V. CONCLUDING REMARKS

To summarize, we have quantitatively analyzed the spatial distribution of Rydberg excitations in the stationary state of resonantly driven, dissipative atomic ensembles. Using an exact numerical solution of the density-matrix equations for a small system, we have shown that the steady state of a strongly interacting multiatom system can be accurately and efficiently simulated by a semiclassical Monte Carlo algorithm if the atoms experience strong dephasing. The semiclassical treatment, however, amounts to an uncontrolled approximation in the case of purely coherent driving of radiatively broadened dipoles. We have considered the dipole-dipole and van der Waals interactions and found that a well-defined blockade distance and a density wave of Rydberg excitations can be observed only in the case of the van der Waals interatomic potential, whereas the dipole-dipole potential is too soft for the emergence of a pronounced density wave. For van der Waals interacting atoms, the steady-state probabilities of Rydberg

excitations exhibit quasicrystallization and damped spatial oscillations whose inverse wavelength and correlation length grow with the probability of collective Rydberg excitations of superatoms which increases with the atomic density and thereby the cooperativity of the excitations. We have presented an approximate, analytically solvable model of incoherently driven Rydberg atoms interacting via a hard-rod potential. Detailed comparison with the results of Monte Carlo simulations justified the hard-rod model but also revealed its limitations for an accurate description of the long-range correlations of Rydberg excitations.

The system studied in this paper corresponds to an ensemble of cold alkali atoms excited to the strongly interacting Rydberg states $|r\rangle$ with a principal quantum number $n \sim 50$–100. The resonant atomic excitation is affected by either direct one-photon (UV) transition $|g\rangle \rightarrow |r\rangle$ or two-photon transition via nonresonant intermediate state [26]. Typical values for the driving field Rabi frequency $\Omega \sim 10^5$ Hz, together with the relaxation rates $\Gamma_r \lesssim 0.1\Omega$ and $\Gamma_z \simeq \Omega$, lead to a blockade distance in the range of $d_b \sim 5$–10 μm. The low-density ensemble of equidistant atoms is trapped in a 1D optical lattice. At higher densities, regular arrangement of the atoms in a lattice would play a minor role, and our results should hold also in the continuous gas of atoms confined in an elongated trap with transverse dimension much smaller than the blockade distance. After sudden switching off of the driving field, the spatial distribution of Rydberg excitations can survive for tens or hundreds of microseconds and can be detected *in situ* by spatially resolved Rydberg state ionization [27] or high-resolution fluorescence imaging [25].

ACKNOWLEDGMENTS

Financial support of the DFG through SFB TR49 is acknowledged. D.P. is grateful to the University of Kaiserslautern for hospitality and support.

[1] T. F. Gallagher, *Rydberg Atoms* (Cambridge University Press, Cambridge, 1994).
[2] M. D. Lukin, M. Fleischhauer, R. Côté, L. M. Duan, D. Jaksch, J. I. Cirac, and P. Zoller, Phys. Rev. Lett. **87**, 037901 (2001).
[3] D. Tong, S. M. Farooqi, J. Stanojevic, S. Krishnan, Y. P. Zhang, R. Côté, E. E. Eyler, and P. L. Gould, Phys. Rev. Lett. **93**, 063001 (2004).
[4] K. Singer, M. Reetz-Lamour, T. Amthor, L. G. Marcassa, and M. Weidemüller, Phys. Rev. Lett. **93**, 163001 (2004).
[5] T. Vogt, M. Viteau, J. Zhao, A. Chotia, D. Comparat, and P. Pillet, Phys. Rev. Lett. **97**, 083003 (2006).
[6] R. Heidemann, U. Raitzsch, V. Bendkowsky, B. Butscher, R. Löw, L. Santos, and T. Pfau, Phys. Rev. Lett. **99**, 163601 (2007).
[7] E. Urban, T. A. Johnson, T. Henage, L. Isenhower, D. D. Yavuz, T. G. Walker, and M. Saffman, Nat. Phys. **5**, 110 (2009); A. Gaëtan, Y. Miroshnychenko, T. Wilk, A. Chotia, M. Viteau, D. Comparat, P. Pillet, A. Browaeys, and P. Grangier, *ibid.* **5**, 115 (2009).
[8] Y. O. Dudin, L. Li, F. Bariani, and A. Kuzmich, Nat. Phys. **8**, 790 (2012).
[9] D. Petrosyan and K. Mølmer, Phys. Rev. A **87**, 033416 (2013).
[10] D. Comparat and P. Pillet, J. Opt. Soc. Am. B **27**, A208 (2010).
[11] M. Saffman, T. G. Walker, and K. Mølmer, Rev. Mod. Phys. **82**, 2313 (2010).
[12] R. Löw, H. Weimer, U. Krohn, R. Heidemann, V. Bendkowsky, B. Butscher, H. P. Büchler, and T. Pfau, Phys. Rev. A **80**, 033422 (2009).
[13] H. Weimer, R. Löw, T. Pfau, and H. P. Büchler, Phys. Rev. Lett. **101**, 250601 (2008).
[14] H. Weimer and H. P. Büchler, Phys. Rev. Lett. **105**, 230403 (2010).
[15] J. Schachenmayer, I. Lesanovsky, A. Micheli, and A. J. Daley, New J. Phys. **12**, 103044 (2010).
[16] I. Lesanovsky, Phys. Rev. Lett. **106**, 025301 (2011).
[17] E. Sela, M. Punk, and M. Garst, Phys. Rev. B **84**, 085434 (2011).
[18] T. Pohl, E. Demler, and M. D. Lukin, Phys. Rev. Lett. **104**, 043002 (2010).
[19] R. M. W. van Bijnen, S. Smit, K. A. H. van Leeuwen, E. J. D. Vredenbregt, and S. J. J. M. F. Kokkelmans, J. Phys. B **44**, 184008 (2011).
[20] G. Pupillo, A. Micheli, M. Boninsegni, I. Lesanovsky, and P. Zoller, Phys. Rev. Lett. **104**, 223002 (2010).
[21] S. Ji, C. Ates, and I. Lesanovsky, Phys. Rev. Lett. **107**, 060406 (2011).
[22] I. Lesanovsky, Phys. Rev. Lett. **108**, 105301 (2012).
[23] C. Ates and I. Lesanovsky, Phys. Rev. A **86**, 013408 (2012).
[24] M. Viteau, M. G. Bason, J. Radogostowicz, N. Malossi, D. Ciampini, O. Morsch, and E. Arimondo, Phys. Rev. Lett. **107**, 060402 (2011).
[25] P. Schauß, M. Cheneau, M. Endres, T. Fukuhara, S. Hild, A. Omran, T. Pohl, C. Gross, S. Kuhr, and I. Bloch, Nature (London) **491**, 87 (2012).
[26] R. Löw, H. Weimer, J. Nipper, J. B. Balewski, B. Butscher, H. P. Büchler, and T. Pfau, J. Phys. B **45**, 113001 (2012).
[27] A. Schwarzkopf, R. E. Sapiro, and G. Raithel, Phys. Rev. Lett. **107**, 103001 (2011).
[28] M. Robert-de-Saint-Vincent, C. S. Hofmann, H. Schempp, G. Günter, S. Whitlock, and M. Weidemüller, Phys. Rev. Lett. **110**, 045004 (2013).
[29] M. Gärttner, K. P. Heeg, T. Gasenzer, and J. Evers, Phys. Rev. A **86**, 033422 (2012); arXiv:1203.2884.
[30] K. P. Heeg, M. Gärttner, and J. Evers, Phys. Rev. A **86**, 063421 (2012).
[31] M. Höning, D. Muth, D. Petrosyan, and M. Fleischhauer, Phys. Rev. A **87**, 023401 (2013).
[32] F. Robicheaux and J. V. Hernandez, Phys. Rev. A **72**, 063403 (2005).
[33] J. Stanojevic and R. Côté, Phys. Rev. A **80**, 033418 (2009).
[34] J. Honer, R. Löw, H. Weimer, T. Pfau, and H. P. Büchler, Phys. Rev. Lett. **107**, 093601 (2011).
[35] C. Ates, T. Pohl, T. Pattard, and J. M. Rost, Phys. Rev. A **76**, 013413 (2007).
[36] C. Ates, S. Sevinçli, and T. Pohl, Phys. Rev. A **83**, 041802(R) (2011).

[37] Z. W. Salsburg, R. W. Zwanzig, and J. G. Kirkwood, J. Chem. Phys. **21**, 1098 (1953); A. Robledo and J. S. Rowlinson, Molec. Phys. **58**, 711 (1986).

[38] We assume the static DD interaction between the atoms in Rydberg states possessing permanent dipole moments induced by an external dc electric field [1].

[39] C. Boisseau, I. Simbotin, and R. Côté, Phys. Rev. Lett. **88**, 133004 (2002); K. Singer, J. Stanojevic, M. Weidemüller, and R. Côté, J. Phys. B **38**, S295 (2005).

[40] P. Lambropoulos and D. Petrosyan, *Fundamentals of Quantum Optics and Quantum Information* (Springer, Berlin, 2007), Chap. 4.